

# Design of a stable fixed delay interferometer prototype for the ET project

Suvrath Mahadevan<sup>a</sup>, Jian Ge<sup>a</sup>, Curtis DeWitt<sup>a</sup>, Julian van Eyken<sup>a</sup> and Gerald Friedman<sup>a</sup>

<sup>a</sup>Pennsylvania State University, 525 Davey Lab, University Park, USA;

## ABSTRACT

The ET instrument being developed at Penn State is a novel approach that is capable of precision radial velocity measurements using a modest resolution. A prototype version of this instrument is now set up permanently at the Kitt Peak 2.1m telescope and has recovered the radial velocity curve of 51 Peg. The stability of the Michelson interferometer used in the setup is very crucial to obtain accurate velocity results. In this paper we discuss the issues associated with field widening and temperature compensation over a wide wavelength range and also describe the design of a prototype interferometer that meets these criteria. Our current prototype design built in the lab already outperforms our old interferometer over short time spans. A new interferometer based on the prototype will replace our current actively stabilized interferometer at Kitt Peak. The increased stability will enable us to start our planet search program in 2005, and to observe targets suitable for asteroseismology.

**Keywords:** Radial Velocity, planets, interferometer, field widening

## 1. INTRODUCTION

The Exoplanet Tracker (ET) instrument is the pilot project for a future all sky radial velocity survey instrument capable of simultaneously observing many hundreds of nearby F-M stars with  $m_v = 7 - 12$  at a precision of 3-20m/s on a wide field of view telescope such as Sloan or WIYN. ET has already demonstrated high short term Doppler precision and stability and has reproduced the RV curves of 51 Peg and Eta Cas.<sup>1</sup> Details of the instrument and future plans are discussed in these proceedings in papers by van Eyken and Ge. Traditional methods to accurately measure radial velocity variations have focused on high resolution cross-dispersed echelle spectrographs, allowing single object spectroscopy. The ET design is a Michelson interferometer with a fixed-delay coupled to a medium resolution post-disperser.<sup>2</sup> Interferometric fringe phase shifts are used to measure velocity instead of absorption line centroid shifts (like in the echelle spectrographs) and the post-disperser exists only to increase the fringe visibility. In this paper we will discuss the design and performance of our new stable interferometer design which keeps the path length drift below an acceptable threshold. The Doppler precision of the instrument is directly linked to the stability of the interferometer. Previous passive stable interferometers have already proven their ability to make precise astrophysical measurements<sup>3,4</sup> (e.g. the GONG project that studies solar oscillations and has demonstrated sub m/s velocity precision). Our interferometer design has a significantly wider bandpass (approximately 2000 Å) than previous interferometer designs to increase its sensitivity for observing stars as faint as 12<sup>th</sup> magnitude at 2-3m class telescopes. To increase stability the interferometer configuration has no active parts. A slight tilt on one of the mirrors enables one to record slightly different delays onto the detector simultaneously and measure the fringe phase without resorting to stepping the phase manually. In contrast to our previous design that uses active control, the emphasis of this new design will be on minimizing path length drifts, and measuring the path differences very accurately to compensate for any residual drifts. Unlike a high resolution spectrograph, where many factors can mimic radial velocity variation, the dominant factor in our case is likely the interferometer path length that can be measured and quantified extremely accurately. A variation of this stable interferometer configuration is also likely to be used in the future multi-object RV survey. This method allows us to stack hundreds of spectra on a CCD mosaic. The orders of magnitude gain in survey efficiency will allow hundreds of thousands of stars to be monitored annually with a single telescope. Initial monitoring of this large sample will be done with the multi-object instrument and targets showing variability will be more intensively followed with higher RV precision by the KPNO ET instrument. Such

---

Further author information: (Send correspondence to Suvrath Mahadevan)  
E-mail: suvrath@astro.psu.edu, Telephone: 814 863 7948

an instrument will also be able to do precise measurements of stellar pulsation, which are relatively insensitive to long term drifts, but require very high stability over a few nights.

## 2. THE ET INTERFEROMETER

The interferometer in the ET setup creates fringes in the starlight. The shift in doppler velocity due to radial velocity variations from the star leads to a change in phase of these sinusoidal fringes. A medium resolution spectrograph placed after the interferometer serves to increase the fringe visibility and record the spectra onto a CCD.

The ET Michelson interferometer is made of BK7 glass and is currently designed to have a delay of 14000 waves at  $\lambda = 500\text{nm}$  (7mm of delay). While this is not necessarily optimal, we will assume here that the 7mm delay at the specified wavelength is what we wish to work with. The interferometer arm of length  $L_1$  has a refractive index of  $n_1$  and the arm of length  $L_2$  has a refractive index of  $n_2$ . The interferometer delay is then given by

$$\Delta = 2(n_1L_1 - n_2L_2) \tag{1}$$

The transmission of such an interferometer can then be written as

$$I = \cos^2\left(\frac{\pi\Delta}{\lambda}\right) \tag{2}$$

The transmitted intensity is then maximum whenever  $\frac{\Delta}{\lambda} = N$ , where N is an integer. For the ET interferometer with 7mm of optical delay at  $0.5\mu\text{m}$  the transmission pattern is illustrated in Figure 1 for a small wavelength band.

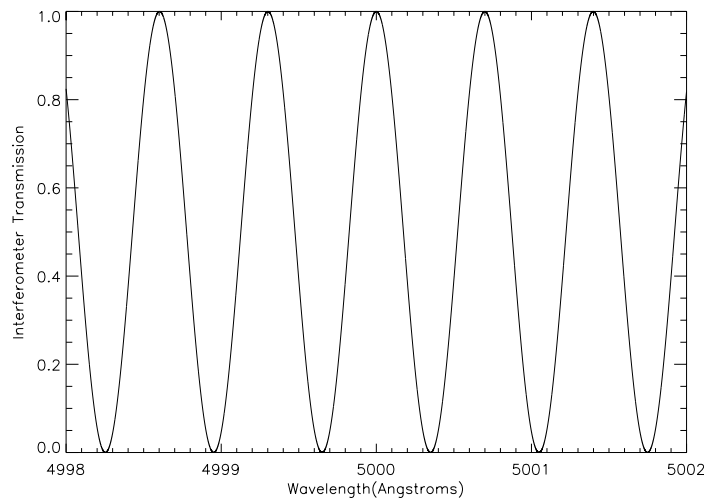


**Figure 1.** Transmission Function for the ET interferometer which has 14000 waves of delay at  $0.5\mu\text{m}$

### 2.1. Crucial Differences from Other Interferometer used in Precision Velocity Measurements

To the best of our knowledge, the ET instrument is the only interferometer based system that has successfully reproduced the radial velocity curve of a planet bearing star. Polarizing cube designs are usually used for helioseismology, but are too inefficient and too narrow in bandwidth to allow the collection of enough velocity information for faint targets (ie.  $m_v < 8^{th}$  magnitude stars). We are therefore using a wide bandpass and a

interferometer that is relatively insensitive to polarization state. This results in some major differences from interferometers used in helioseismology, or to measure atmospheric phenomena, that essentially look at one absorption or emission line.

1. Bandwidth: Unlike other projects that only need narrow bandwidths of 0.01-0.1nm, we actually need the instrument to be workable from 400-600nm where the bulk of the velocity information is found in F, G, and K stars. The current ET instrument set up at the KPNO 2.1m telescope is currently designed for a 60nm wavelength range centered on 520nm, but we plan to expand this in the near future.
2. Beam-splitter Coating: The Beam-splitter coating is not a polarizing coating. We just want to split the incident light so that fringing occurs. Over the required bandwidth we would like to have the splitting as close to a 50-50 split, and as efficient as possible.
3. Deliberate Waves of Tilt: Some designs use a PZT device or a rotating polarizer to change the delay. We have chosen to accomplish the same by putting a few waves of tilt (4 vertical waves at  $0.53\mu\text{m}$  over 1cm of aperture.) This way we have an interferometer with no moving parts, making it easier to stabilize and maintain the accuracy of the delay.
4. Optical Contacting : Epoxies used to join up the components might exhibit some level of creep as the epoxy shrinks. To avoid this we prefer to have the elements optically contacted to make the assembled system as stable as possible. The current prototype is held together with mechanical pressure instead of using epoxies.

## 2.2. Interferometer Tilt : Recording the Phase Information

Let the optical delay of the interferometer be  $d$ , the interferometer can then be described in terms of the interference order  $m$  where

$$m\lambda = d \quad (3)$$

A change in radial velocity shifts the wavelength of an absorption line in the spectrum by an amount  $\Delta\lambda$

$$\Delta m = \frac{d}{\lambda^2} \Delta\lambda \quad (4)$$

If we now use the Doppler shift formula and use the phase ( $\phi = 2\pi m$ ) we can express the change in velocity as a change in observed phase

$$\Delta v = \frac{c\lambda}{2\pi d} \Delta\phi \quad (5)$$

So we can retrieve the velocity shift if we know the delay and the phase of the interferometer. To obtain phase information requires changing the delay by a few waves using a PZT or a GONG type design that scans using a rotating polarizer. We have decided to implement the few waves of delay directly on our interferometer by tilting one mirror of the Michelson. This has the advantage of having no movable parts, as well as being able to record all the phase information simultaneously. For the ET instrument our current design calls for 4 waves of tilt over 1 cm of aperture (See Fig 3). These interferometer fringes are then imaged onto the spectrograph slit, and recorded on the CCD after dispersion. The two dimensional image formed is then used to estimate the phase of every wavelength. A change in velocity manifests itself as a vertical phase shift of the sin waves in the spectra. Since the interferometer arms terminate in mirrors, we can put a tilt on one mirror causing it to exhibit 4 waves of path difference ( $4 \times 0.5\mu\text{m} = 2\mu\text{m}$ ) over 1cm of aperture in the vertical direction. Due to the double pass the actual physical offset of the mirror only has to be  $1\mu\text{m}$  over the 1cm aperture. This translates to a tilt of only 21 arcseconds on the mirror itself.

### 3. FIELD WIDENING: DECREASING SENSITIVITY OF INTERFEROMETER PATH DIFFERENCE TO INPUT ANGLE

The path difference of a normal Michelson interferometer is a very strong function of the input angle. This is unacceptable for a number of applications and it is possible to achieve field widening by choosing the materials and lengths in both arms carefully. Field widening has been discussed in detail by Hillard and Shepherd<sup>5</sup> and we briefly present here the relevant calculations and apply them to our particular design.

#### 3.1. Field Compensation

For a ray entering an interferometer at an arbitrary angle  $i$  the delay ( $\Delta$ ) is given by

$$\Delta = 2[n_1 L_1 (1 - \frac{\sin^2 i}{n_1^2})^{-\frac{1}{2}} - n_2 L_2 (1 - \frac{\sin^2 i}{n_2^2})^{-\frac{1}{2}}] \quad (6)$$

If we expand all the terms of  $\sin i$  till the fourth order and ignore higher order terms, we get

$$\Delta = 2[(n_1 L_1 - n_2 L_2) - \frac{\sin^2 i}{2} (\frac{L_1}{n_1} - \frac{L_2}{n_2}) - \frac{\sin^4 i}{8} (\frac{L_1}{n_1^3} - \frac{L_2}{n_2^3})] \quad (7)$$

The  $\sin^2 i$  term in the equation for the delay can be set to zero by setting

$$\frac{L_1}{n_1} = \frac{L_2}{n_2} \quad (8)$$

This process of choosing length of the arms and materials to give the needed delay, while making the second order angle term zero, is known as field compensation since it allows a much larger acceptance angle for the interferometer. The delay for a compensated interferometer then becomes

$$\Delta = \Delta_0 [1 + \frac{\sin^4 i}{8n_1^2 n_2^2}] \quad (9)$$

Where  $\Delta_0$  is the interferometer delay ie.  $i = 0$  or when the ray is along the axis of the interferometer. The half angle of acceptance is sometimes defined as the angle where the change in delay from  $i = 0$  amounts to a phase shift of a half wave, depending on the particular constraints of the instruments the angle  $i$  at which the interferometer is still useful can then be determine. We calculate the variation in phase caused by the the change in incident angle for an uncompensated interferometer, a fully compensated interferometer and a partially compensated interferometer (Figure 2 and 3). We calculate this over a 3 degree half angle, which is twice the ET interferometer acceptance angle. For the ET instrument a 200mm focal length cylindrical lens converges the 1cm beam along one axis. This translates to an angle in air of about 1.45 degrees.

#### 3.1.1. Uncompensated Michelson Interferometer

For an uncompensated interferometer made with air delays in both legs, we can write the variation in optical delay as a function of angle as

$$\Delta = \Delta_o [1 - \frac{(\sin(i))^2}{2} + \frac{(\sin(i))^4}{24}] \quad (10)$$

Using this we find that for a 7mm delay at 500nm the uncompensated interferometer has 19.1 waves of phase change over the 3 degree half angle, and 4.5 waves over the 1.5 degree ET field(See Figure 2). Obviously, this is totally unacceptable and will work only if the beam is very slow or nearly collimated. Even for a collimated beam, it is preferable to have some level of field compensation to reduce the constraints on how good the collimation has to be.

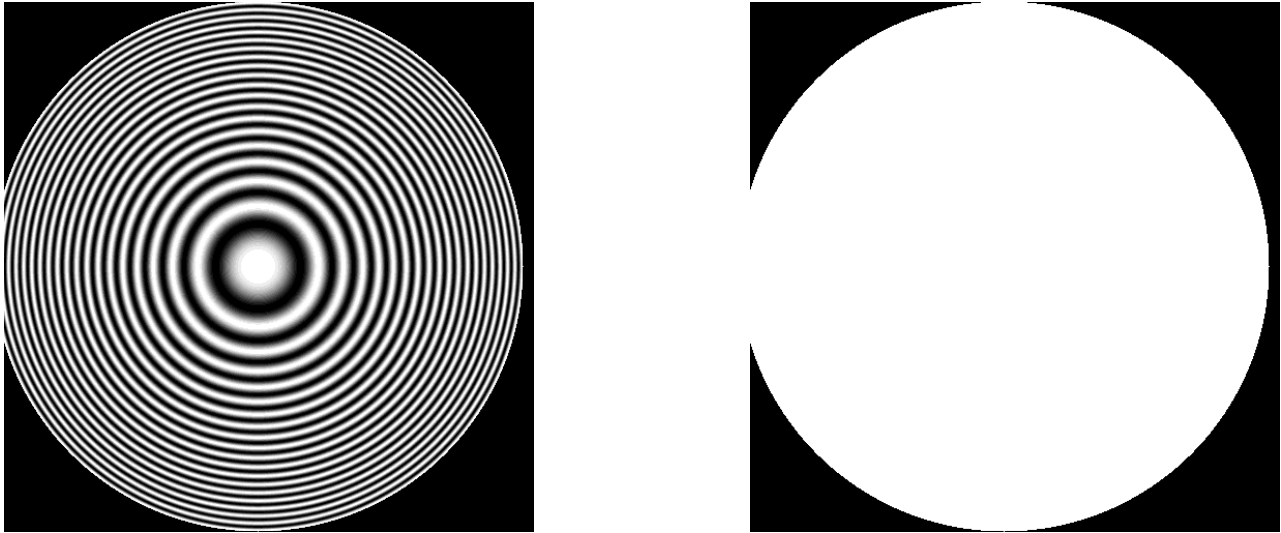


**Figure 2.** Phase variation across a 3 deg half angle a) for an uncompensated and b) a fully compensated Michelson interferometer. Compare the 40 waves of phase change for the uncompensated Michelson with the complete absence of any visible phase changes in the fully compensated interferometer

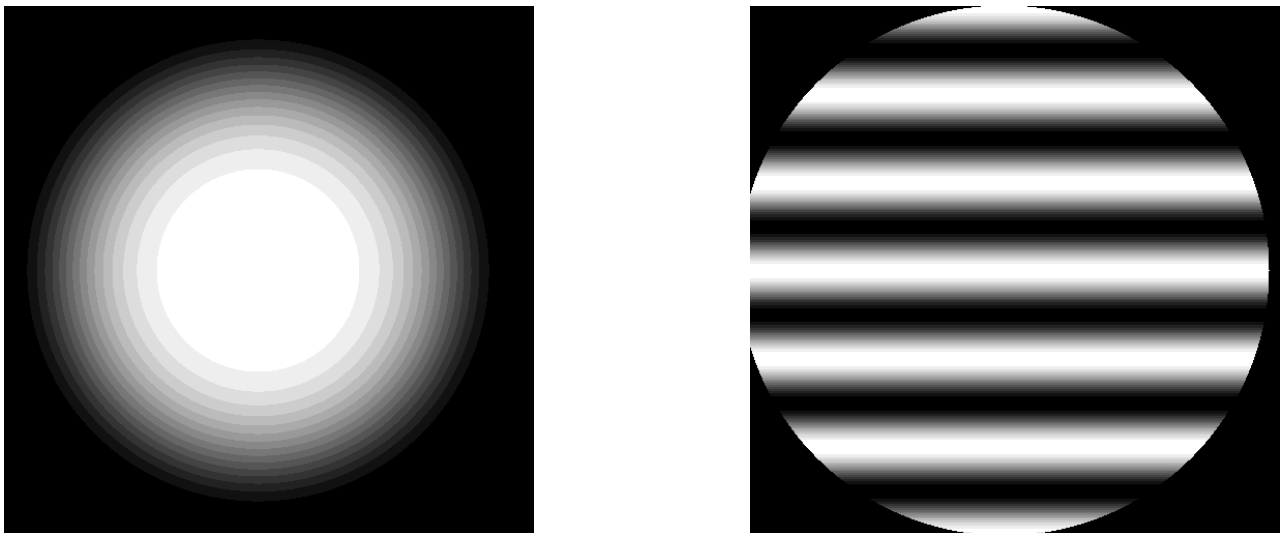


**Figure 3.** a) Phase variation across a 3 degree half angle for a partially compensated interferometer where the air arm is  $100\mu\text{m}$  off from the perfect compensation condition. b) Waves introduced by tilting one mirror of a well compensated interferometer

### 3.1.2. Fully Compensated Michelson Interferometer

For a Michelson interferometer with one arm made of BK7 and the other arm having an air space we can calculate the arm lengths needed for perfect field compensation and a delay of 7mm (or 14000 waves) at 500nm. These numbers turn out to be

BK7 Glass Arm=4.040mm  
 AIR Space Arm=2.662mm

Its important to recognize here that the lengths have been chosen to make the  $\sin^2$  term in the delay disappear. Even more field widening can be achieved by choosing the lengths so that partial cancellation of the  $\sin^2$  and  $\sin^4$  terms takes place, but we deem this to be unimportant for us since we have a rather small half angle as it is. For the fully compensated interferometer at 500nm the variation in phase turns out to be  $5.67 \times 10^{-3}$  waves for 3 degrees.

Complete field compensation has only been achieved at the design wavelength of 500nm. This wavelength has no special interest other than being at the center of our range of interest. The interferometer must also perform well at other wavelengths from 400nm-600nm. To evaluate the performance we define a term  $\epsilon$  which is a measure of how much the interferometer parameters are different from those required for the field widened condition

$$\epsilon = \frac{L_1}{n_1} - \frac{L_2}{n_2} \quad (11)$$

Recall that choice of arm lengths has been made such that the delay is 7mm and  $\epsilon = 0$  at 500nm. We then calculate the value of  $\epsilon$  at every wavelength keeping the arm lengths and the refractive index of air ( $n_{air} = 1.0$ ) constant while calculating the refractive index of BK7 at each wavelength using the Sellmeier dispersion formula. The field compensation is seen to be off by  $-16\mu\text{m}$  in the blue to  $8\mu\text{m}$  in the red over the wavelength range 400-600nm. A non-zero  $\epsilon$  means that the interferometer is no longer perfectly field compensated for that wavelength. The shift in phase from the original delay(which is different for different wavelengths) can be calculated using the value of  $\epsilon$ . We find that the maximum deviation of phase over wavelength is 0.12 waves for the 3 degree half angle and 0.03 waves for the 1.5 degree half angle.

### 3.1.3. Partially Compensated Michelson Interferometer

Even with precise aligning of the interferometer, and custom machining of the legs it is not possible to achieve exactly the fully compensated condition. Any optical mismatch will basically be equivalent to having a non-zero value of  $\epsilon$ . We have explored the effect of deliberately introducing a large value of  $\epsilon$  at 500nm where it is supposed to be zero. We change the length of the air arm by  $100\mu\text{m}$ . This leads to a change in phase of 0.55 waves over the 3 degree half angle. This is a very large difference from the compensation condition and is calculated just as an illustration. It does serve to point out that the machining and alignment tolerances must be under  $10\mu\text{m}$  for the lengths of the interferometer arms.

## 4. TEMPERATURE COMPENSATION: DECREASING SENSITIVITY OF THE INTERFEROMETER TO TEMPERATURE DRIFTS

Field compensation allows the path difference to not be a strong function of the angle, however the total path difference can still change with temperature due to the thermal expansion and the dependance of refractive indices on temperature. This changing path difference will mimic a radial velocity variation if it is not controlled. Title and Ramsey<sup>6</sup> built a birefringent element from a polarizing wide field interferometer and demonstrated how a proper choice of material could minimize temperature sensitivity. The phase of a beam going through the interferometer can be written as

$$\phi = \frac{2\pi}{\lambda}(n_1 d_1 - n_2 d_2) \quad (12)$$

We can then calculate  $d\phi/d\lambda$  and  $d\phi/dT$ . Using these, the wavelength sensitivity of a fully compensated Michelson interferometer can be written as

$$\frac{d\lambda}{dT} = \frac{-\lambda n_1^2 [n_1^2 (\frac{1}{n_1} \frac{dn_1}{dT} + \frac{1}{L_1} \frac{dL_1}{dT}) - n_2^2 (\frac{1}{n_2} \frac{dn_2}{dT} + \frac{1}{L_2} \frac{dL_2}{dT})]}{(n_1^2 - n_2^2) [1 - \frac{n_1^2 \lambda}{(n_1^2 - n_2^2)} (\frac{1}{n_1} \frac{dn_1}{d\lambda} - (\frac{n_2}{n_1})^2 \frac{1}{n_2} \frac{dn_2}{d\lambda})]} \quad (13)$$

Therefore, the compensated interferometer is completely insensitive to temperature fluctuations when

$$n_1^2 (\frac{1}{n_1} \frac{dn_1}{dT} + \frac{1}{L_1} \frac{dL_1}{dT}) - n_2^2 (\frac{1}{n_2} \frac{dn_2}{dT} + \frac{1}{L_2} \frac{dL_2}{dT}) = 0 \quad (14)$$

The derivatives of refractive index with respect to wavelength can easily be calculated with the Sellmeier dispersion formula, while the derivatives of refractive index with temperature can be calculated using the Sellmeier Formula for  $dn/dT$ .

Calculating this using standard values for air and refractive index variations and using copper as a spacer element gives a value of 16.75 mÅ for the change in wavelength over a 1 degree change in temperature. This translates to a velocity change of 1 km/s for each degree centigrade that the temperature shifts. To keep the shifts under 1 m/s the temperature has to be stable to 1 mK or better. Alternatively, we can work on reducing the effect of the temperature by choosing a better spacer material than copper (Another possibility is to enclose the interferometer in a vacuum, thereby removing the dependence on the air refractive index). For this analysis we have used values that are approximate, or analytical, but one wants to use the measured values to calculate the correct results. The temperature dependence can change rapidly even with small changes in the refractive indices used, nevertheless, using the copper spacer with air arms improves the temperature dependence by almost an order of magnitude compared to a BK7 spacer.

## 5. THE PROTOTYPE INTERFEROMETER: CURRENT PERFORMANCE AND FUTURE PLANS.

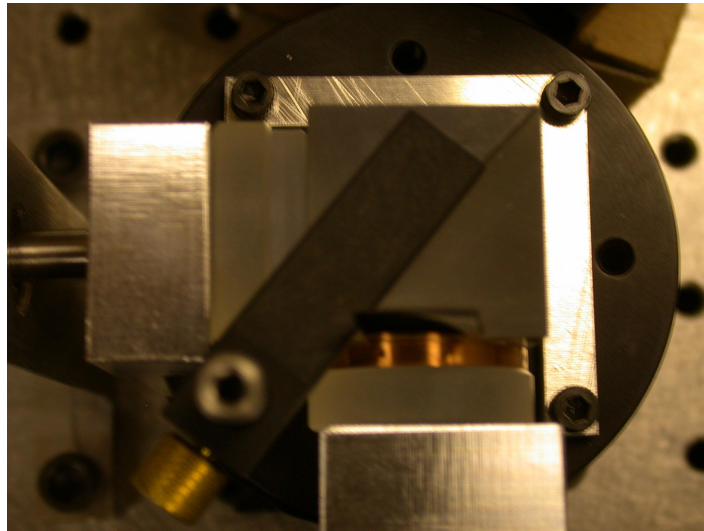


**Figure 4.** The Prototype interferometer built at Penn State for testing out the field widening and temperature stability. The copper spacer in one arm of the interferometer is clearly visible

We have constructed a prototype interferometer using a commercially available BK7 beamsplitter and mirrors. One arm of the Michelson interferometer is a 4mm BK7 etalon, and the other is a copper ring machined to be a thickness of 2.66mm. The interferometer was set up in lab and is held together by mechanical pressure using custom made mounts. The stability of the interferometer was tested by passing laser light from a single mode fiber (for complete scrambling) through the interferometer and imaging the fringes. The recorded fringe drifts are all attributed to the varying path difference of the interferometer due to small temperature changes and flexures. No attempt was made to control the temperature of this interferometer. The results from this experiment were quite encouraging. The interferometer was almost perfectly field compensated, and was stable to  $\lambda/5000$  over a few seconds, although longer term drifts are seen. This is better than we have ever achieved in our lab before. The long term drifts are likely due to temperature changes and flexure from the micrometers used to pressure contact the interferometer parts.

A newer version of this interferometer is being designed to exhibit less temperature dependence. This new interferometer is scheduled to be tested at Kitt Peak in November 2004 and will replace our current actively stabilized interferometer if it works. The instrument room at Kitt Peak is quite stable, and the RMS temperature

variation at the location of our current interferometer is only 0.03 Celsius (see Figure 5). The ET instrument room is located at the base of the coude spectrograph room, and is quite stable. The thick walls of the room provide insulation from the external temperature variation, and a heater and fan keep the internal room temperature at a fixed point. The instrument itself lies on a optical bench in this room, and has another layer of sealed insulation panels around it.

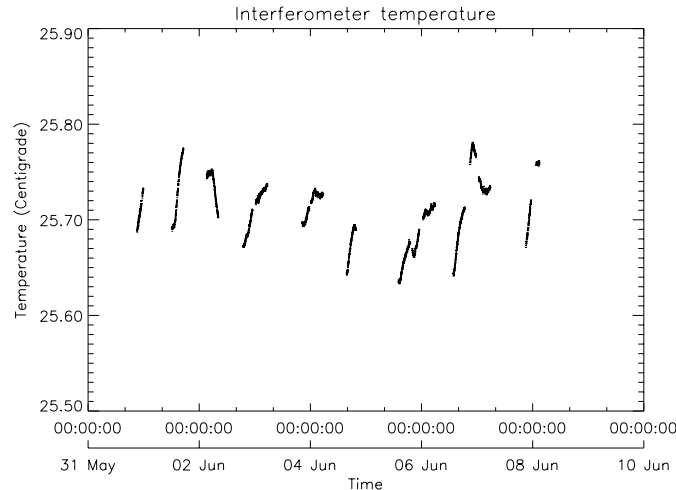


**Figure 5.** Temperature variability of the current ET interferometer at Kitt Peak during an observing run

## 6. CONCLUSION

The high resolution-throughput product of interferometers makes them useful for a variety of innovative instruments, but great care is needed in understanding the requirements. Precision radial velocity measurements push existing instruments to their limits, and second order effects become important. In this paper we have discussed a strategy to minimize the effect of input angle and temperature variations on the velocity measured. A stable interferometer will allow the ET instrument to perform long term radial velocity surveys, as well as asteroseismology. On a longer timescale, the ET instrument at the KPNO 2.1m will be opened to the general users, and a stable interferometer is transparent to the user and easier to use, unlike an actively controlled one which needs almost continuous user intervention.

This work would not have been possible without an interesting and insightful discussion with Jack Harvey at NSO. SM would like to acknowledge the Michelson Fellowship for support. JVE and SM would like to thank NOAO for providing travel support to Kitt Peak. We would also like to thank the staff at KPNO for their effort in making this project possible.

## REFERENCES

1. J. C. van Eyken, J. Ge, S. Mahadevan, and C. DeWitt, "First Planet Confirmation with a Dispersed Fixed-Delay Interferometer," **600**, pp. L79–L82, Jan. 2004.
2. J. Ge, "Fixed Delay Interferometry for Doppler Extrasolar Planet Detection," *ApJ* **571**, pp. L165–L168, June 2002.
3. J. Harvey and The GONG Instrument Team, "The GONG Instrument Michelson Interferometer," in *ASP Conf. Ser. 76: GONG 1994. Helio- and Astro-Seismology from the Earth and Space*, pp. 432–+, 1995.
4. I. E. Kozhevnikov, E. K. Kulikova, and N. P. Cheragin, "An integrating interference spectrometer," *Astronomy Letters* **21**, pp. 418–422, May 1995.

5. R. L. Hilliard and G. G. Shepherd, "Wide-Angle Michelson Interferometer for Measuring Doppler Line Widths," *JOSA* **56**, pp. 362–371, 1966.
6. A. M. Title and H. E. Ramsey, "Improvements in Birefringent Filters. VI. Analog Birefringent Elements," **19**, pp. 2046–2058, 1980.